# Thermal Convection in a Closed Water Body wit Aquatic Plants

Hamagami, Kunihiko
Graduate School of Bioresource and Bioenvironmental Schiences, Kyushu University

Mori, Ken
Faculty of Agriculture, Kyushu University

Hirai, Yasumaru
Faculty of Agriculture, Kyushu University

https://doi.org/10.5109/9249

出版情報：九州大学大学院農学研究院紀要. 51 (2), pp.323-329, 2006-10-27. Faculty of Agriculture, Kyushu University
バージョン：
権利関係：

J. Fac. Agr., Kyushu Univ., **51** (2), 323–329 (2006)

# Thermal Convection in a Closed Water Body with Aquatic Plants

**Kunihiko HAMAGAMI[1], Ken MORI*, and Yasumaru HIRAI**

Laboratory of Bioproduction and Environment Information Sciences, Division of Bioproduction and Environment Information Sciences, Department of Bioproduction and Environmental Science, Factory of Agriculture, Kyusyu University, Fukuoka 812–8581, Japan
(*Received June 30, 2006 and accepted July 24, 2006*)

In some closed water bodies with little inflow and outflow, because the flow is gentle, hydraulic characteristics are different from a river or an irrigation canal. When there is no disturbance, fluid is stratified based on vertical density distribution. In these bodies, the main dynamics of the water environmental substance depends on the wind current on a water surface induced by the mechanical disturbance and a convective flow induced by a thermal disturbance. We focused on a convective flow induced by the thermal disturbance. The mechanism of the generation and development processes of the gravity convection by surface cooling was investigated through the numerical experiment and the hydraulic experiment for the closed water body covered with aquatic plants. As the results, a density difference was generated horizontally because of the coverage of the water surface, and the horizontal convection was caused. This effect influenced the development speed of convection cells in a vertical direction, and the development speed of a mixture layer has increased.

## INTRODUCTION

When there is no disturbance in some closed water bodies with little inflow and outflow, water mass which contains a generous quantity of DO on the surface is not easily transported to a lower layer. Therefore, the poverty of oxygen happens around a bottom layer, and it leads the water quality deteriorations and eutrophication. Then, it is necessary to understand fluid flow characteristics of the water bodies to examine the improvement and the maintenance of water quality.

As circulation sources in a closed water body, there are a mechanical disturbance due to wind action on a water surface and thermal disturbance due to radioactive cooling from a water surface. We focused on a convective flow induced by the thermal disturbance. Many studies suggest that gravitational convection plays an important role in heat transportation, material transportation and water mass formation in a shallow sea (Imasato *et al*., 1978; Shay and Gregg, 1986; Suga *et al*., 1989). Akitomo (1991) explained mechanisms of the generation and development processes of gravity convection due to surface cooling in a shallow sea. In this study, the numerical analysis and the hydraulic experiment were conducted, in order to examine characteristics of a density current due to water surface cooling in a closed water body covered with aquatic plants.

## METHODS AND RESULTS

### Hydraulic experiment

*Experiment purpose*

A vertical convection phenomenon by thermal convection is influenced by the scale of the heat flux of water surface cooling. The change in vertical distribution of water temperature due to water surface cooling with elapse time was measured under various coverage rates of water surface. The present experiment was conducted under both conditions of thermal uniformity and thermal stratification.

*Experiment equipment*

The test tank was made of acrylic plates (length＝20 cm, width＝10 cm, depth＝20 cm) (cf. Fig. 1). The bottom and sides of the test tank were covered with styrene foam boards of 20 mm in thickness to prevent heat radiation. A thermocouple was used to measure water temperature. Thermocouples were set in a vertical direction at 1 cm intervals, starting at 0.5 cm from the water surface. The location of 0.5 cm from the water surface was defined as the water surface in this experiment. Air temperature was measured by a mercury thermometer.

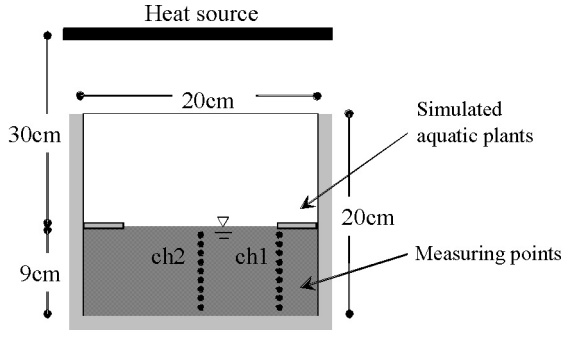


**Fig. 1.** Experimental equipment.

[1] Laboratory of Bioproduction and Environmental Information Sciences, Division of Bioproduction and Environment Sciences, Department of Bioproduction Environmental Sciences, Graduate School of Bioresource and Bioenvironmental Sciences, Kyushu University

* Corresponding author (E–mail: moriken@bpes.Kyushu–u.ac.jp)

*Experimental method*

The present experiment was conducted by using the small scale test tank in which air temperature was not controlled. For the experiment under thermal stratification, the fluid was heated from 30 cm above the water surface with the electric heat board (GRIDDLE–SL 5, 100 V–12 A) for two hours, and then the fluid was naturally cooled from the water surface for two hours. Thermal uniformity was formed by pouring hot water (approximately 100 degrees Celsius) into water in the tank and stirring them, and then the fluid was cooled under the same condition as the experiment under thermal stratification.

The vertical distribution of water temperature was measured at the point of 3 cm from the sidewall (ch 1) and at the center of the test tank (ch 2) (c.f. Fig. 1). The sampling frequency was 0.5 Hz. The air temperature was measured at the location of 1m away from the test tank. In the experiment, the effect of the vegetation was investigated under four coverage ratios on the water surface: 0%, 20%, 40%, and 60%. Simulated plants made from polystyrene form plates were used instead of using real aquatic plants. The plates of 5 mm in thickness were set on the water surface at both ends of the test tank. The experimental conditions are shown in Table 1.

*Experimental results and discussions*

Figure 2 shows the calorie of the water column per unit area at the location of ch 1. Under thermal stratification, the calorie was increased during the heating process, and decreased during the cooling process. Moreover, the rate of change was large at the condition

**Table 1.** Experimental conditions of the hydraulic experiment

| Exp | fluid condition | coverage ratio | measuring duration (h) | initial temperature at a water surface $T_w$ (°C) | initial air temperature $T_a$ (°C) | $\Delta T = T_w - T_a$ (°C) |
|---|---|---|---|---|---|---|
| 1–1 | stratification | 0% | 4 | 21.8 | 12.0 | 9.8 |
| 1–2 | stratification | 10% | 4 | 20.2 | 9.0 | 11.2 |
| 1–3 | stratification | 30% | 4 | 21.3 | 11.0 | 10.3 |
| 1–4 | stratification | 50% | 4 | 20.1 | 10.0 | 10.1 |
| 2–1 | uniformity | 0% | 2 | 17.7 | 8.8 | 8.9 |
| 2–2 | uniformity | 10% | 2 | 19.7 | 10.8 | 8.3 |
| 2–3 | uniformity | 30% | 2 | 17.9 | 9.5 | 8.4 |
| 2–4 | uniformity | 50% | 2 | 17.4 | 8.4 | 9.0 |

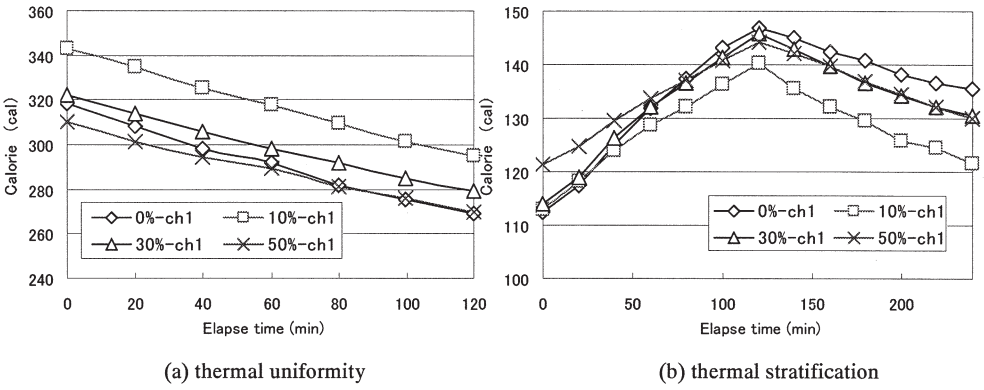


**Fig. 2.** Time variation of the calorie of the water column per unit area.

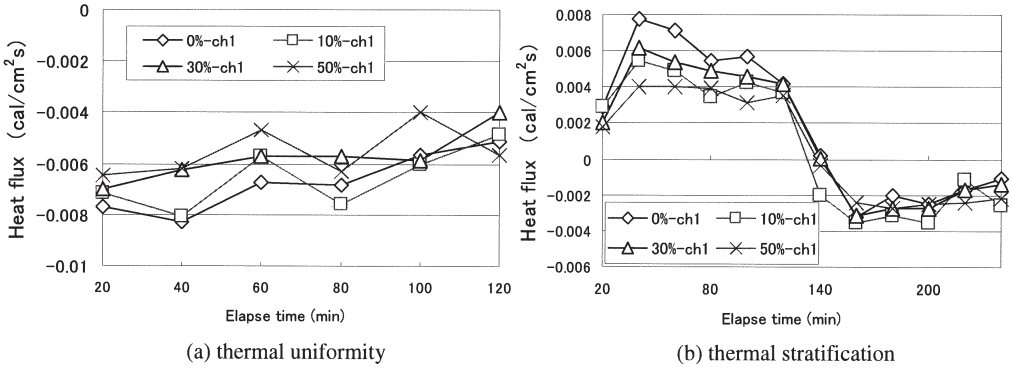


**Fig. 3.** Time variation of the heat flux per unit water surface area.

without coverage during both heating and cooling processes. A similar tendency was seen for the rate of change during a cooling process under thermal uniformity.

Figure 3 shows the heat flux per unit water surface area at the location of ch1. Under thermal stratification, the heat flux rose rapidly by 30 minutes of elapse time and gradually decreased during a heating process. During cooling process, the heat flux took a negative value because the direction of the heat transfer changed. Afterwards, the value gradually approached to zero because the difference between the water temperature and the air temperature became small. As well as the calorie, the heat flux and its rate of change were large in the case of 0% coverage. A similar tendency was also seen under thermal uniformity during a cooling process.

Table 2 shows Rayleigh numbers as one of the experimental conditions. The Rayleigh number is defined as

$$R_a = \frac{\alpha g \Delta T h^3}{\kappa \nu} = \frac{\alpha g q h^4}{\rho C_p \kappa^2 \nu} \quad (1)$$

where $\alpha$ is coefficient of thermal expansion (1/℃); $\Delta T$, temperature difference between air and water temperature (℃); $h$, water depth (cm); $\kappa$, thermometric conductivity (cm²/s); $\nu$, coefficient of kinematics viscosity (cm²/s); $q$, heat flux (cal/cm²•s); $\rho$, reference density (g/cm³); $C_p$, specific heat (cal/g•℃); and $g$, gravitational acceleration (cm/s²). The parameters in Eq(1) were defined as $\alpha = 2.5 \times 10^{-4}$, $g = 980$, $\kappa = 1.4 \times 10^{-4}$, and $\nu = 0.01$.

Brunt–Vaisala Frequency $N$ shows the stability of stratification, and it is called the stability frequency. Figure 4 shows the time evolution of $N$ at the location of ch 2 (the center of the test tank) under thermal stratification. The values of $N$ around the thermal interface were large at the beginning of the cooling process. And they vertically became uniform as time elapsed. This

**Table 2.** Rayleigh number at each experimental condition

| Exp | fluid condition | coverage ratio | $\Delta T$ (℃) | Heat Flux $q$ (cal/cm²s) ch 1 | ch 2 | Rayleigh numbers $R_a$ ch 1 | ch 2 |
|---|---|---|---|---|---|---|---|
| 1–1 | stratification | 0% | 9.8 | 6.33E−03 | 8.40E−03 | 5.19E+10 | 6.89E+10 |
| 1–2 | stratification | 10% | 11.2 | 6.50E−03 | 7.38E−03 | 5.33E+10 | 6.05E+10 |
| 1–3 | stratification | 30% | 10.3 | 7.58E−03 | 8.35E−03 | 6.22E+10 | 6.85E+10 |
| 1–4 | stratification | 50% | 10.1 | 5.79E−03 | 7.15E−03 | 4.75E+10 | 5.86E+10 |
| 2–1 | uniformity | 0% | 8.9 | 8.62E−03 | 7.71E−03 | 7.07E+10 | 6.32E+10 |
| 2–2 | uniformity | 10% | 8.3 | 7.04E−03 | 7.17E−03 | 5.78E+10 | 5.88E+10 |
| 2–3 | uniformity | 30% | 8.4 | 6.58E−03 | 7.00E−03 | 5.40E+10 | 5.74E+10 |
| 2–4 | uniformity | 50% | 9.0 | 7.13E−03 | 6.46E−03 | 5.84E+10 | 5.30E+10 |

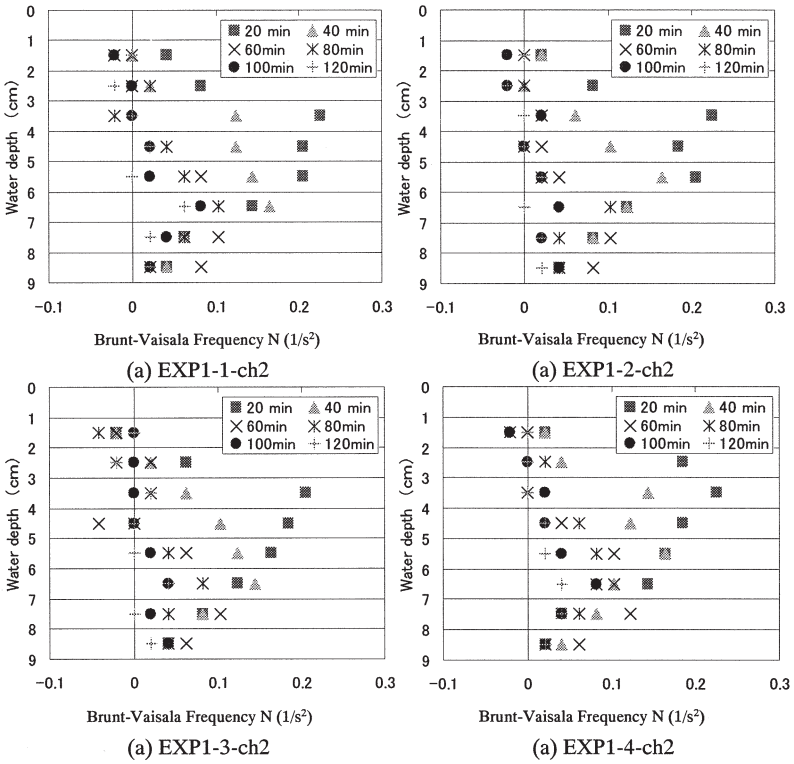


**Fig. 4.** Time variation of Brunt–Vaisala Frequency $N$.

result shows that the thermal uniformity was lead by the elimination of thermal stratification. And depth of the peak value increased as time elapsed. This shows the development stage of the mixture layer, and is thought that the stratification stability around the bottom of the mixture layer was high. Moreover, as the coverage increased, the change speed in the peak location of $N$ became small.

Figure 5 shows total hydraulic pressure $P$ under thermal stratification and thermal uniformity. Pressure in depth $z$ (cm) is $\rho gz$ (g/cm$\cdot$s$^2$) and total hydraulic pressure $P$ is calculated by the following formula;

$$P=\int_0^H \rho gz\, dz \tag{2}$$

where $H$ is water depth. It is obtained by the numerical integral with the trapezoidal rule. The increase rate of pressure started to decrease in about 80 minutes under thermal stratification. This is thought that the development of convection was interrupted by the influence of the density stratification. Next, when the value of $P$ in ch 1 and ch 2 were compared, the pressure difference among them was large. When there is a pressure difference in a water body, water flows from a high pressure side to a low pressure side to eliminate pressure difference and then the horizontal flow is caused.

**Numerical experiment**

*Governing equations of heat convection*

Figure 6 shows the calculation area. We assumed the simple rectangle water body where 9 cm in depth $H$ and 20 cm length $L$. The $x$ axis was set in a horizontal direction, and the $z$ axis directs upward. Governing equations of a Boussinesq fluid motion in a two–dimensional rotating frame under rigid–lid approximation are the equation of continuity (3), the dynamic equation ((4), (5)), the temperature diffusion equations (6), and the equation of density–temperatures (7).

$$\frac{\partial u}{\partial x}+\frac{\partial w}{\partial z}=0 \tag{3}$$

$$\frac{\partial u}{\partial t}+u\frac{\partial u}{\partial x}+w\frac{\partial u}{\partial z}=-\frac{1}{\rho_0}\frac{\partial p}{\partial x}+\upsilon_x\frac{\partial^2 u}{\partial x^2}+\upsilon_z\frac{\partial^2 u}{\partial z^2} \tag{4}$$

$$\frac{\partial w}{\partial t}+u\frac{\partial w}{\partial x}+w\frac{\partial w}{\partial z}=-\frac{1}{\rho_0}\frac{\partial p}{\partial z}-\frac{\rho}{\rho_0}g+\upsilon_x\frac{\partial^2 w}{\partial x^2}+\upsilon_z\frac{\partial^2 w}{\partial z^2} \tag{5}$$

$$\frac{\partial T}{\partial t}+u\frac{\partial T}{\partial x}+w\frac{\partial T}{\partial z}=K_x\frac{\partial^2 T}{\partial x^2}+K_z\frac{\partial^2 T}{\partial z^2} \tag{6}$$

$$\rho=\rho_0(1-\alpha T) \tag{7}$$

where $u$ and $w$ are the velocity in $x$ and $z$ directions; $p$, pressure deflection from hydrostatic pressure at the constant density $\rho_0=1\,g/cm^3$. ($p$ is assumed to be only a function of temperature); $\alpha$, coefficient of thermal expansion ($2\times10^{-4}$°C$^{-1}$); $\upsilon_x$ and $\upsilon_z$, horizontal and vertical eddy viscosities; $K_x$ and $K_z$, the horizontal and vertical eddy diffusivities. The pressure inclination is included in these equations. Because a clear equation to obtain the pressure is not given in the above equations, stream function $\psi$ ($u=\partial\psi/\partial z$, $w=-\partial\psi/\partial x$) and vorticity $\zeta$ are considered as shown in Eq (8).

$$\zeta=-\left(\frac{\partial^2\psi}{\partial x^2}+\frac{\partial^2\psi}{\partial z^2}\right) \tag{8}$$

After elimination of $p$ from Eq (4) and (5), Eq (4), (5) and (7) are transformed into Eq (9)

$$\frac{\partial\zeta}{\partial t}+u\frac{\partial\zeta}{\partial x}+w\frac{\partial\zeta}{\partial z}=\alpha g\frac{\partial T}{\partial x}+\upsilon_x\frac{\partial^2\zeta}{\partial x^2}+\upsilon_z\frac{\partial^2\zeta}{\partial z^2} \tag{9}$$

Figure 6 shows boundary conditions at the model area. The insulated and no–slip boundary conditions are assumed at bottom and both sides ($z=0$ and $x=0, L$). The constant flux for water temperature and free–slip boundary conditions are assumed at surface ($z=H$).

$$u_{x=0}=w_{x=0}=0,\ \left.\frac{\partial T}{\partial x}\right|_{x=0}=0 \tag{10}$$

$$u_{x=L}=w_{x=L}=0,\ \left.\frac{\partial T}{\partial x}\right|_{x=L}=0 \tag{11}$$

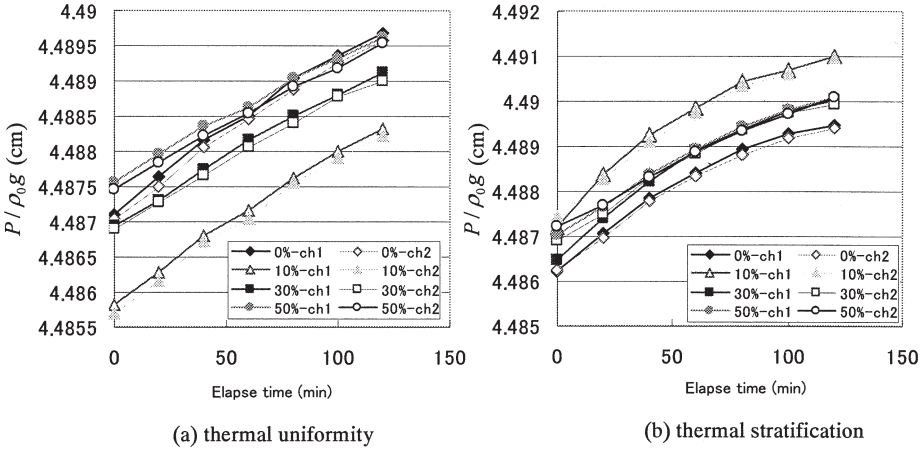


(a) thermal uniformity (b) thermal stratification

**Fig. 5.** Time variation of all hydraulic pressure $P$.

$$u_{z=0}=w_{z=0}=0,\ \left.\frac{\partial T}{\partial z}\right|_{z=0}=0 \tag{12}$$

$$\left.\frac{\partial u}{\partial z}\right|_{z=H}=w_{z=H}=0,\ \left.\frac{\partial T}{\partial z}\right|_{z=H}=-q \tag{13}$$

The coverage ratio of the aquatic plants on the water surface was changed with 0%, 10%, 30%, and 50% under thermal stratification and uniformity. Heat flux is expected to become small because of the low degree of the heat conductivity of vegetation at the covered areas.

$$q_{\mathrm{cov}}\,erd=\beta\cdot q\ (\beta<1) \tag{14}$$

where $\beta$ is a coefficient multiplied by $q$ in the covered part, and it was assumed $\beta=1/3$ from the experimental results.

Values of constant physical parameters are tabulated in Table 3. The previous study suggests that anisotropic property of eddy diffusivity causes the horizontal scale to be larger than the vertical one by a factor $\sqrt{K_x / K_z}$ where $K_x(K_z)$ is the horizontal (vertical) eddy diffusivity (Priestly,1962; Ray,1965). Therefore, the horizontal and vertical component of eddy viscosity and eddy diffusivity were decided considering effect of advection.

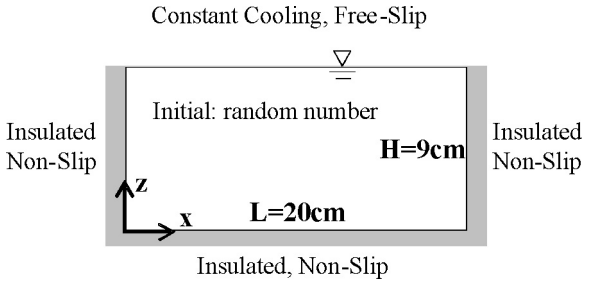


**Fig. 6.** Model basin with boundary and initial conditions.

**Table 3.** Values of constant parameters used in the calculation

| | | |
|---|---|---|
| horaizontal eddy viscosities | $\nu_x$ | $1.0\mathrm{cm^2s^{-1}}$ |
| Vertical eddy viscosities | $\nu_z$ | $0.01\mathrm{cm^2s^{-1}}$ |
| horizontal eddy diffusivities | $K_x$ | $1.0\mathrm{cm^2s^{-1}}$ |
| Vertical eddy diffusivities | $K_z$ | $0.01\mathrm{cm^2s^{-1}}$ |
| Heat flux | $q$ | $-0.005\mathrm{ly\cdot s^{-1}}$ |
| Thermal expansion coefficient | $\alpha$ | $2.1\times10^{-4}\mathrm{^\circ C^{-1}}$ |
| Horizontal grid length | $\Delta x$ | 0.5cm |
| Vertical grid length | $\Delta z$ | 0.5cm |
| Calculating step | $\Delta t$ | 0.1s |

**Table 4.** Experimental conditions of numerical calculation

| RUN | fluid condition | coverage ratio | calculating during (h) | initial temperature at a water surface (°C) |
|---|---|---|---|---|
| 1–1 | stratification | 0% | 2 | 21.0 |
| 1–2 | stratification | 10% | 2 | 21.0 |
| 1–3 | stratification | 30% | 2 | 21.0 |
| 1–4 | stratification | 50% | 2 | 21.0 |
| 2–1 | uniformity | 0% | 2 | 17.7 |
| 2–2 | uniformity | 10% | 2 | 17.7 |
| 2–3 | uniformity | 30% | 2 | 17.7 |
| 2–4 | uniformity | 50% | 2 | 17.7 |

The conditions of numerical calculation are shown in Table 4. RUN1 assumed thermal stratification, and the vertical distribution of water temperature was set at the same conditions as EXE1–1 in hydraulic experiment when the water surface cooling started. RUN2 assumed thermal uniformity, and the initial temperature was set at the same conditions as EXE2–1. Calculated basin initially was given random numbers as a trigger of fluid motion.

*Development process of convection cells*

Figure 7 shows the temperature distribution and the stream function under thermal uniformity without coverage. As beginning of water surface cooling ($t=$ 3 min), the thermal boundary layer is formed beneath the water surface and became thickened gradually. Moreover, the stream line is minute disturbance given as an initial condition, and remarkable convection is not caused (Fig. 7(a)). At $t=10$ min, the boundary layer finally breaks down and a multitude of small–scale convection cells appear in the whole water body. The number of them reaches 18 (Fig. 7(b)). When the cold water mass falls in thermal and a plain convection cell is formed it can be called an initial stage of mixture layer development. At $t=15$ min, the mergence of these cells begins and the horizontal scales of surviving cells become larger (Fig. 7(c)). This stage, where the convection cell absorbs or annexes, and the horizontal scale is increased, can be called a transient stage. The convection cell becomes two pairs at $t=30$ min, and continues a comparatively steady state afterwards. It can be called quasi–steady stage (Fig.7(d)). The water temperature distribution shape at this time resembles the distribution of the stream line closely. This shows that convection greatly contributes to the decrease in water temperature.

Figure 8 shows the temperature distribution and the stream function under thermal stratification without coverage. It is important to consider the density interface in the case of thermal stratification. In the vicinity of the density interface, the degree of stability is high, and a large influence can be given on the falling behavior of the cold water mass. When calculating, it is necessary to consider it. Then, the method of deciding the vertical eddy diffusivities according to the Brunt–Vaisala frequency, which shows the stability degree of the stratification, was used.

$$K_z/\upsilon=(1+10^6N4)^{-1} \tag{15}$$

where $N$ is the Brunt–Vaisala frequency.

The development process of convection changes from initial stage to transient stage, and then to quasi–steady stage as well as the case of thermal uniformity. But the development speed of convection is small compared with thermal uniformity. It is at $t=$ 27 min that the stability of the density interface collapses and the convection cell reaches the lower layer (Fig. 8(c)). That is, it can be said that the development of convection is obstructed by the density interface. In

the numerical experiment duration until vertical scale of convection cell reaches bottom layer under thermal stratification is twice as long as the case of thermal uniformity.

Figure 9 shows development of mixture layer at each coverage rate. In the numerical experiment at this time, the middle point between maximum water temperature and a minimum water temperature was defined at the bottom of the mixture layer. The development speed of the mixture layer increases obviously compared with the case without coverage. That is, shortening time for collapse of the stability of the density interface described in the previous paragraph appears as a difference at the development speed of the mixture layer. Though the difference by coverage ratio is not clear, the development speed of the mixture layer has a tendency to decrease when the rate of the coverage is increased.

The influence of the coverage was examined in detail by considering the term balance of the vorticity equation. Fig. 10 shows the comparison about the term balance of the vorticity equation in the upper layer (2 cm in depth) at $t=18$ min for each coverage ratio (0%, 10%, 30%, 50%). The dotted line in the figure

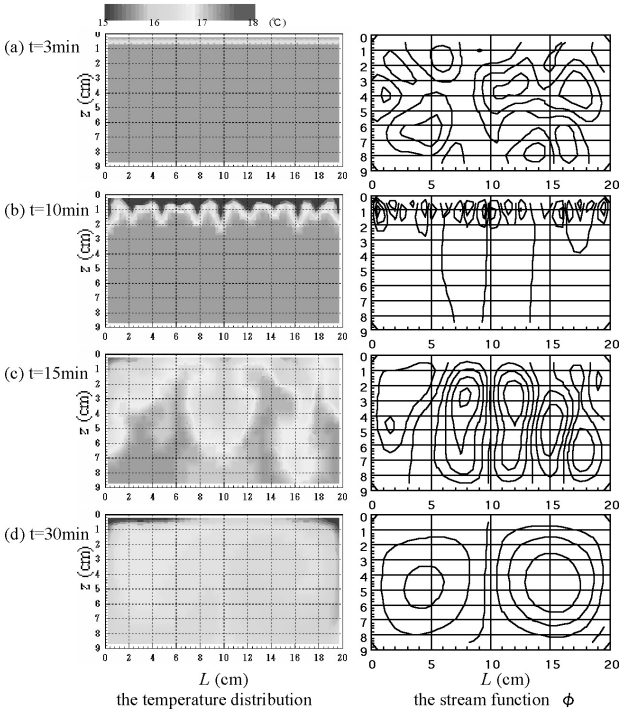


**Fig. 7.** The temperature distribution and the stream function under thermal uniformity without coverage.

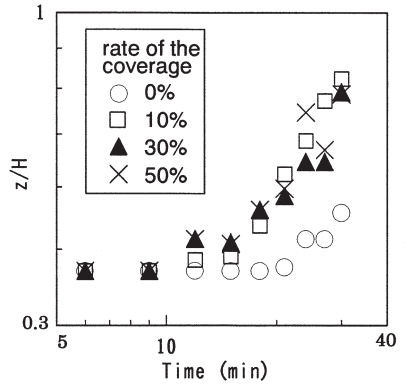


**Fig. 9.** Time variation of the development of mixture layer.

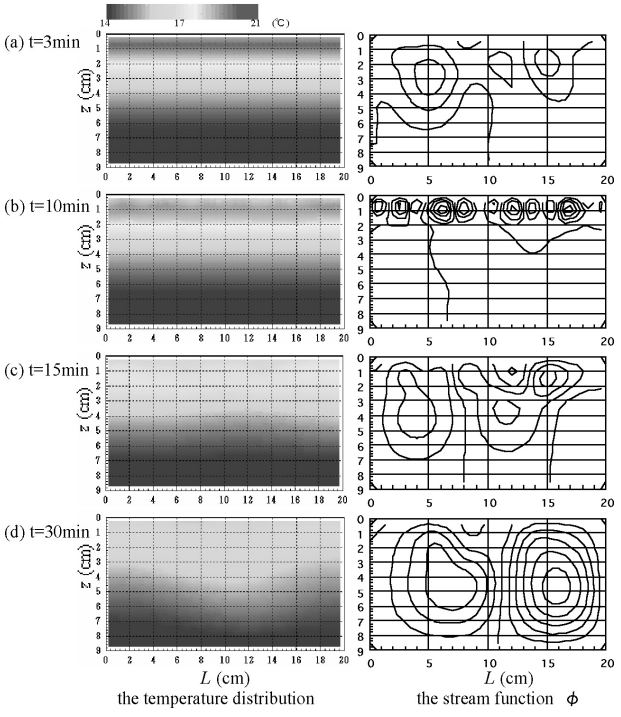


**Fig. 8.** The temperature distribution and the stream function under thermal stratification without coverage.

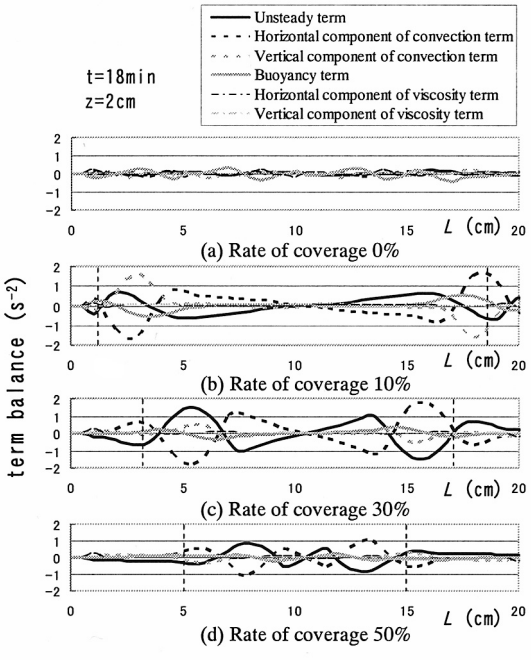


**Fig. 10.** Term balance of the vorticity equation at each rate of coverage.

shows the edge of the coverage. The contribution of each term is growing compared with the case without coverage. Especially, the horizontal component of convection term is superior in the vicinity of the edge of the coverage. That is, the contribution of the horizontal convection is greatly related to the increase of the development speed of the convection cell by coverage on the water surface.

## CONCLUSION

In this study, the process of the water surface cooling was reproduced based on the water tank experiment and the numerical experiment concerning generation and development of the heat convection, and the following results were obtained about the influence of aquatic plants in the water body.

(1) Generation and development process of heat convection by the water surface cooling is classified into initial stage where a multitude of small convection cells are generated, transient stage where the horizontal scale of the convection cell is increased, and quasi–steady stage where the convection cell continues a comparatively steady state afterwards.

(2) The density stratification obstructs the development of a vertical scale of convection with the role of the heat transportation. In the numerical calculation, the effect was expressed as function of the Brunt–Vaisala frequency, therefore the development speed in the vertical direction became about half.

(3) Density difference was formed horizontally because of the coverage of the water surface, and the horizontal convection was caused. This effect influences the development speed of the convection cell in a vertical direction, and the development speed of the mixture layer increased.

## ACKNOWLEDGEMENTS

The authors wish to thank Laboratory of Drainage and Water Environment, Division of Regional Environmental Science, Department of Bioproduction Environment Science, Faculty of Agriculture, Kyushu University for the convenience in the conducting the experiment.

## REFERENCES

Akitomo, K., N. Imasato, S.–I. Yamashita, T. Awaji and G.–Y. Yu 1992 A numerical study on scale selection of convection in a shallow sea. *Continental Shelf Research*, **12**: 451–469

Imasato, N., H. Kunishi, H. Takeoka, H. Yoshioka, T. Yanagi, T. Awaji and S. Endoh 1978 On the variations of general sea conditions in the Seto Inland Sea. *Bulletin of Coastal Oceanography (in Japanese)*, **15**: 138–142

Priestly, C. H. B. 1962 The width–height ratio of large convection cells. *Tellus*, **14**: 123–124

Ray, D. 1965 Cellular convection with nonisotropic eddies. *Tellus*, **17**: 434–439

Shay, T. J. and Gregg, M. C. 1986 Convectively driven turbulent mixing in the upper ocean. *Journal of Physical Oceanography*, **16**: 1777–1798

Suga, T., K. Hanawa and Y. Toba 1989 Subtropical mode water in the 137°E section. *Journal of Physical Oceanography*, **19**: 1605–1618